Investigating Nearshore Surface Currents and Tidal Influences on Marine Debris Deposition on O‘ahu, Hawai‘i

A THESIS SUBMITTED TO
THE GLOBAL ENVIRONMENTAL SCIENCE
UNDERGRADUATE DIVISION IN PARTIAL FULFILLMENT
OF THE REQUIREMENTS FOR THE DEGREE OF

BACHELOR OF SCIENCE

IN

GLOBAL ENVIRONMENTAL SCIENCE

AUGUST, 2021

By
HAN NGOC QUACH

Thesis Advisor

James Potemra, Ph.D

I certify that I have read this thesis and that, in my opinion, it is satisfactory in scope and quality as a thesis for the degree of Bachelor of Science in Global Environmental Science.

THESIS ADVISOR

James Potemra, PhD

Department of Oceanography

For 17-year-old Han, who graduated high school with a 1.9 GPA and could not have fathomed college.

Look how far you've come.

ACKNOWLEDGEMENTS

Throughout the many years of my academic career, I have racked up a slew of people whom I am forever in debt to. First and foremost, I would like to thank my advisor, Dr. Jim Potemra for all of his guidance, patience, and encouragement throughout the course of my thesis. Thank you for making the most challenging aspect of my degree feel like a breeze.

I would also like to thank my family and especially my partner, Shaun Wriston, for their unwavering love and support. Of course, this acknowledgement wouldn't be complete without the GES fam. Thank you to Dr. Michael Guidry and Lentina Villa for their guidance, and all the GES friends-turned-family who have made this long, hectic trip in the GES lounge a memorable one.

A very special thank you to Dr. Wendy Kuntz and Mackenzie Manning of Kapiolani Community College for being there since the very beginning. I wouldn't be where I am now without you two.

ABSTRACT

Marine debris poses great threats to coastal areas and is known to accumulate in large quantities along the shorelines of the Main Hawaiian Islands. However, debris accumulation is not deposited in an even manner. The results of this study show that, 1) seasonal mean forcing does not lead to accurate predictions of the distribution of marine debris along the shorelines of Oʻahu, and 2) surface currents are highly variable and time dependent. Due to high spatial and temporal variability, surface currents during specific events likely play a large role in the uneven spatial distribution of marine debris along the shorelines of Oʻahu.

TABLE OF CONTENTS

LIST OF FIGURES

1.0 Introduction

An estimated 4 to 12 million metric tons of land generated plastic waste entered the marine environment in 2010 alone (Jambeck et al., 2015), and is the main component of marine debris. Historically, the state of Hawaiʻi has the highest reported accumulation of marine debris in all of the United States' Pacific Ocean coastlines (Ribic et al., 2012). Habitat destruction, entanglement and choking hazards as well as the introduction of invasive aquatic species are just some the ways that marine pollution threatens the prosperity of the Hawaiian island's marine ecosystem. In addition to environmental damages, Hawaiʻi's economy is highly susceptible to the negative impacts of marine litter. A study conducted by NOAA showed that beaches with an increase of marine debris received less visitor traffic, thus resulting in the eventual loss of local jobs (English et al., 2019). According to the Hawaiʻi Tourism Agency 2019 report, tourism brought in a total of 17.75 billion dollars' worth of revenue, making it the single largest source of private capital for the state of Hawaiʻi.

Marine debris is transported through the ocean by a wide variety of physical processes. The subtropical North Pacific Ocean is comprised of a system of wind-driven rotating currents dubbed the North Pacific Subtropical Gyre (Howell et al., 2012). Figure 1 shows three significant areas of accumulation that exists within the subtropical gyre: the Western Garbage Patch (WGP), the Eastern Garbage Patch (EGP), and the Subtropical Convergence Zone (SCZ), which is a zone that links the two garbage patches together.

It is speculated that the northeasterly trade winds are the primary drivers that transport floating debris from these convergence zone towards the Main Hawaiian Islands (MHI)

(Blickley et al., 2016; Moy et al., 2018), resulting in the islands receiving large quantities of debris per year (Howell et al., 2012; Ribic et al., 2012).

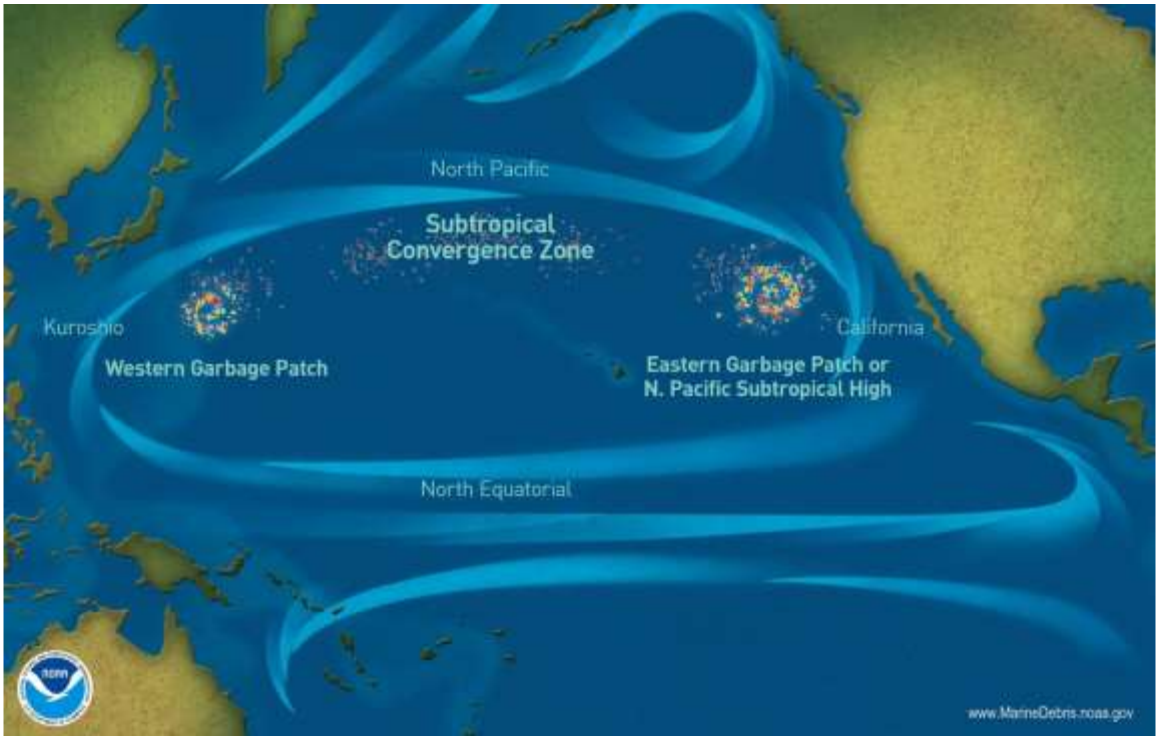

Figure 1. A cartoonish depiction of the North Pacific Subtropical Gyre along with the areas of accumulation.

A survey was published (Moy et al., 2018) that used high-resolution aerial imagery to categorize and quantify marine debris accumulation along coastlines of all eight Main Hawaiian Islands. The survey showed the debris had accumulated in a spatially heterogenous manner, with areas of high debris density often times adjacent to areas with much lower levels of debris, or sometimes no debris at all. It is difficult to reconcile the Moy et al. (2018) findings with the idea of trade winds forcing: if trade winds were the primary reason of marine debris' arrival to the MHI, shouldn't there be a more even distribution of said debris given the fact that trade winds are consistent in direction? Inspired by Moy et al. (2018), we investigated the special distribution of marine debris in the Hawiian Islands in an attempt to explain the patchiness. A particle tracking simulator, OceanParcels (Delandmeter and Sebille, 2019), was used. Our trajectory experiments were forced using output from numerical models. We conducted three sets of experiments including both forward and backward integrations (the former demonstrating where particles go, the latter where they originate), general ocean currents and tidal currents (see Figure 3).

2.0 Background

2.1 Sources, Sinks, and Transportation

More often than not, marine debris is the result of poorly managed waste, be it land derived, or ocean derived. The EPA (2021) reports that 80% of marine litter that are found during beach cleanups can be attributed to trash, packaging and improperly disposed waste from land-based sources. About one-third to two-thirds of catalogued debris from cleanup efforts had come from single-use, disposable packaging. The remaining 20% is made up of lost or abandoned fishing gears as well as deliberate or accidental discharge from nautical vessels.

There are many factors that govern the transportation of marine debris. Figure 2 shows which physical processes (and one biological process) affect particle movements relative to where they are in the ocean. Offshore and at greater depths, large-scale and submesoscales open ocean processes dominates particle transportation. Meanwhile, processes that govern nearshore particles movements are coastal currents, surface waves, and beaching, as well as extreme events. Processes that influence debris transportation regardless of depth or regions are open ocean Stokes drift, internal tides, windage, Langmuir circulation, vertical mixing, ice formations (melting and drifting), river plumes and coastal fronts, and transportation via organisms.

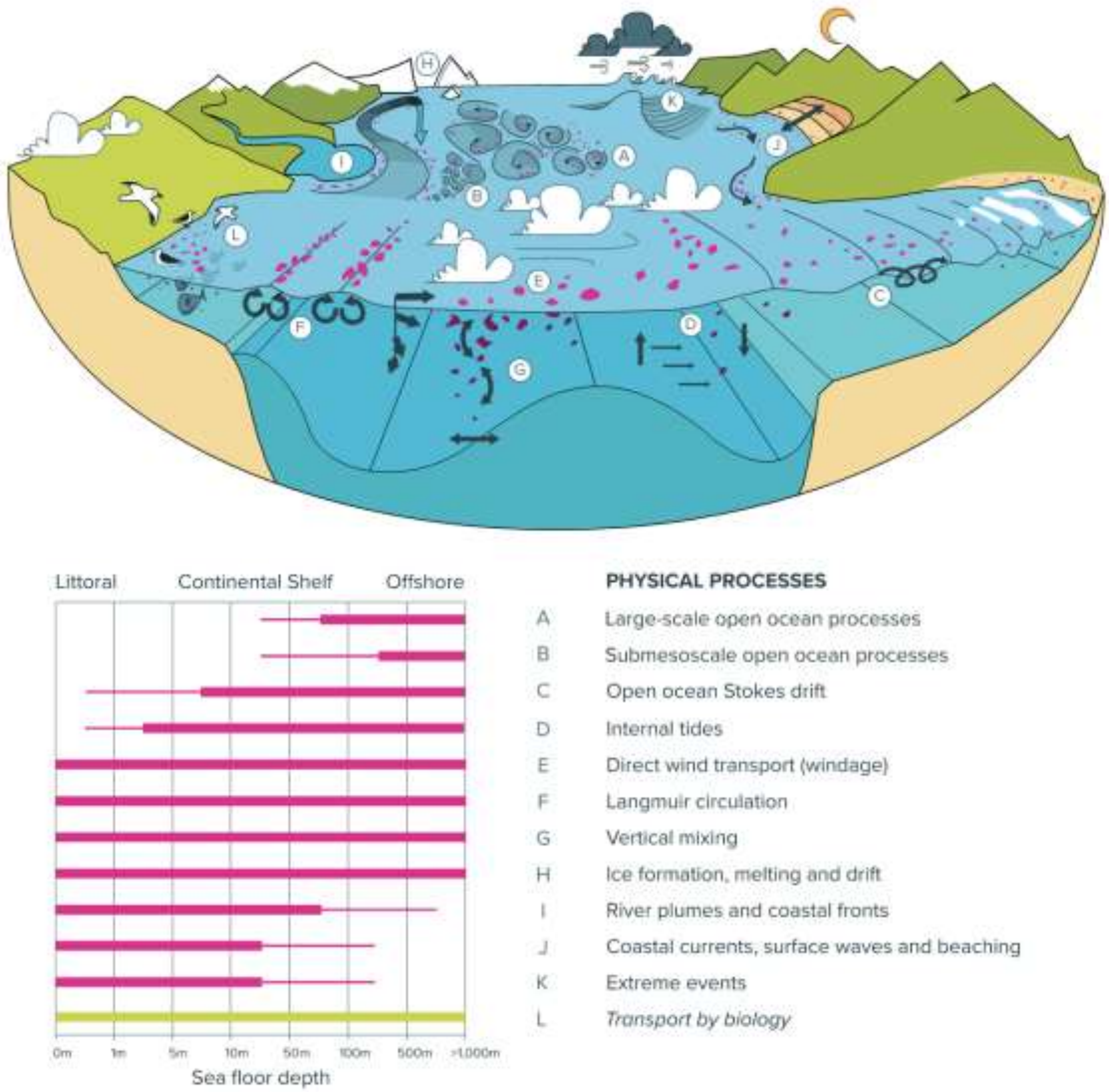

Figure 2. A schematic from van Sebille et al., (2020) of the physical processes that affects the transportation of floating plastic (pink items) in the ocean (top panel). The table below shows which processes are more influential based on which region the plastics are in. The thick pink line in the table indicates that the process is most important, while the thin pink line indicates that the process is of secondary importance. The green line represents transportation done by organisms.

2.2 The Great Tōhoku Earthquake and Tsunami, and the Detrital Aftermath

In March of 2011, a 9.0 magnitude earthquake struck Japan resulting in a tsunami that sent millions of tons of debris into the ocean (Ministry of the Environment, Japan, 2012). In the autumn of 2015, a large-scale aerial survey was conducted by Moy et al. (2018), done in collaboration with the State of Hawaiʻi's Department of Land and Natural Resources (DLNR) and the Hawaiʻi Coral Reef Initiative of the University of Hawaiʻi at Mānoa. This survey mapped the marine debris that had accumulated along the shorelines of the eight Main Hawaiian Islands (MHI) as a result of the tsunami. The study utilized drones to capture high-resolution images to identify a total of 20,650 items of macro debris. However, it is important to note that Moy et al. (2018) study does not differentiate between land-based litter and ocean-based litter and cannot detect small particles of trash.

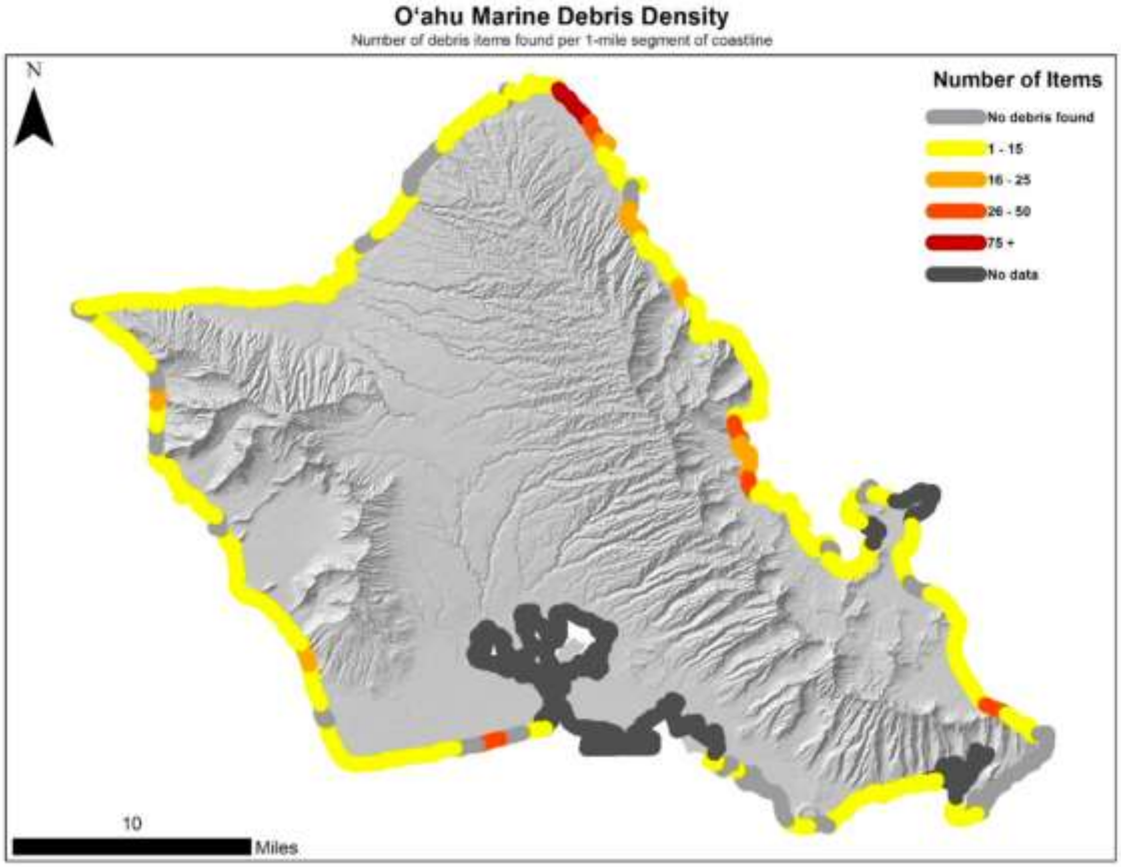

Figure 3. Marine debris density on the shorelines of O‘ahu, Hawai‘i from Moy et al., (2018). Areas labeled ‘No Data’ are due to airspace restrictions (i.e., military bases, airports, etc.)

2.3 Hawai‘i’s Oceanographic Setting and Wave Climate

This section describes the mean wind and ocean patterns surrounding the Hawaiian Islands. The main islands span from 164°W to 153°W longitude and 17°N to 23°N latitude, a region under the direct influence of northeasterly trade winds and swells.

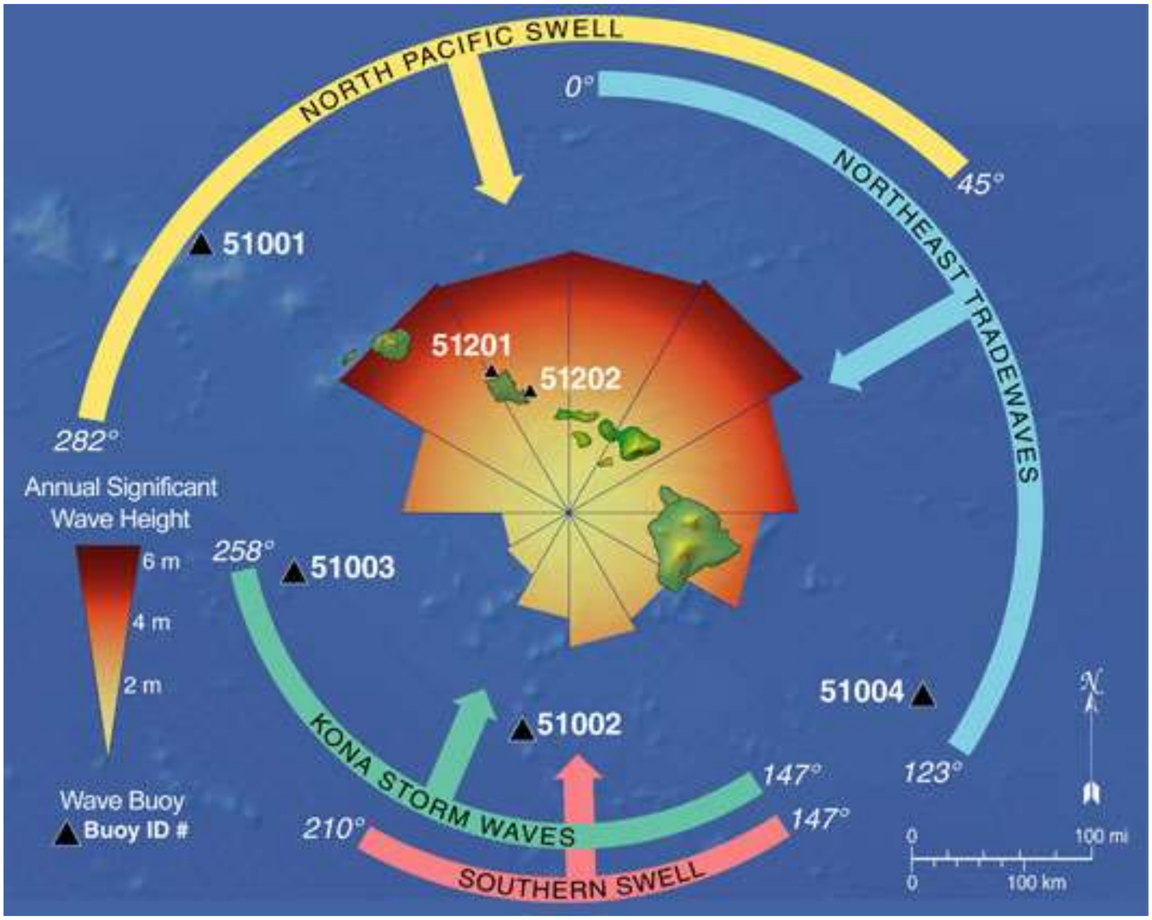

Figure 4. Hawai'i dominant swell regimes after Moberly & Chamberlain (1964), and wave monitoring buoy locations. From Vitousek & Fletcher (2008).

2.3.1 Trade winds and trade wind swell

According to Vitousek et al. (2009), trade winds blow from the Northeast approximately 75% of the year with an average speed of 7 m/s and in the direction of 73° (from northeast to southwest) with a standard deviation of (1σ) of 2.2 m/s and 23°. However, during Northern Hemisphere winter months (Dec, Jan, Feb), there is a decrease in trade wind.

Trade winds generate limited fetch trade wind swells on the northeastern facing coasts with an average height of 2 m and peak periods of 9 sec (Vitousek et al., 2009).

However, trade wind swells can exceed 5 m and have periods for 15-20 sec (Vitousek et al., 2009).

2.3.2 Northern and southern swells

Located in the north Pacific, Hawai‘i sits in the middle of a large swell-generating basin where it recieves large ocean swells from extra-tropical storms that are eastbound from the northwest Pacific (Vitousek et al., 2009). Strong winds associated with these storms create large swell events that can travel for thousands of miles before reaching the Hawaiian shores (Vitousek et al., 2009). On average, winter months recieve wave heights in the north Pacific at approximately ≥ 3 m while the summer wave heights are approximately ≤ 2 m (Vitousek et al., 2009). North Pacific swells have an annual maximun wave height of 7.7m (Vitousek & Fletcher 2008) and a peak period of 1418 sec. However, high variability does exists with respect to size and number of swells per year (Caldwell 2005). Southern swells are generated from storms that exists south of the equator and occur in summer months and have an annual significant wave height of 2.5-3 m and peak periods of 14-22 sec, which are slightly longer than north Pacific swell (Armstrong 1983, Vitousek & Fletcher 2008).

2.3.3 Kona Storms

Kona storms are low-pressure systems that originate in the subtropics in the winter months and slowly travel eastward (Giambelluca and Schroeder, 1998). While minor Kona storms occur practically every year, strong Kona storms can generate wave height of 3-4 m and periods of 8-11 sec with wind and rain possessing the ability to cause extensive damange to the south and west facing shores (Rooney & Fletcher 2005).

2.3.4 Tides

Hawai‘i has mixed, mainly semidiurnal tides, which means that there are two unequal high tides and two unequal low tides per tidal day.The tidal range is relatively small compare to the rest of the world, having an average of 0.58 m and a spring tide range around 1.0 m (Vitousek et al., 2009).

2.3.4

3.0 Data and Methodology

3.1 OceanParcels

OceanParcels (http://www.oceanparcels.org) version 2.0 is a particle tracking simulator that utilzes the Lagrangian ocean anaylsis framework to track the transport of marine litter (Delandmeter and van Sebille, 2019). Particle trajectories are computed using a set of Python classes and methods that can be customized using outputs from ocean circulation models. Outputs from circulation models provide flow fields for particles to be advected by.

Lagrangian particle trajectories are computing using Equation 1.0 (Lange and van Sebille, 2017), where $\boldsymbol{X}$ is the three-dimensional position of a particle, $\boldsymbol{v}(\boldsymbol{x}, t)$ is the three-dimensional velocity field at that location in the ocean model, and $\boldsymbol{X}_b(t)$ is how the particle changes with respect to position due to its “behavior”. Advection of particles are implemented by a fourth-order Runge-Kutta scheme.

$$\mathbf{X}(t+\Delta t) = \mathbf{X}(t) + \int_t^{t+\Delta t} \mathbf{v}(\mathbf{x},\tau)\mathrm{d}\tau + \Delta\mathbf{X}_b(t)$$

Equation 1.0

3.2 Data

For ocean currents, we used output from the Regional Ocean Modeling Systems (ROMS): Main Hawaiian Islands 3D reanalysis developed by the Pacific Islands Ocean Observing System (PacIOOS). PacIOOS ran a 10-year (July 2007 to May 2017), data-assimilating reanalysis for the region surrounding the main Hawaiian Islands at approximately 4-km resolution, 3-hourly interval (Partridge et al., 2019). The domain in which the model covers is between 164°W to 153°W longitude and 17°N to 23°N latitude. The data was assimilated for each day over the previous 3 days using all available observations to improve the model estimate of current ocean state. Boundary conditions for the model was provided by the global, 1/12-degree (~9-km) Hybrid Coordinate Ocean Model. Atmospheric forcing was generated by the Weather Research and Forecasting model at approximately 6-km resolution. Tidal forcings were taken from the Oregon State University Tidal Prediction Software TOPEX/Poseidon global inverse solution to derive barotropic tidal elevation and velocity.

For tidal data, we used both the velocity and the elevation dataset available for the Tide Model for the Hawaiian Islands, also developed by PacIOOS. The model runs at 1-km resolution, hourly, through the end of 2021 (Carter et al., 2008). The model is based on climatological stratification, but 64 harmonics were used to model the full depth baroclinic tides. Due to computing limitation, the model grid was split into two pieces. The one that was used in this study was for the Northwestern Main Hawaiian Islands (O‘ahu, Kaua‘i, Maui).

3.3 Simulation

Three sets of experiments were conducted. These experiments were designed in an attempt to answer two questions: 1) where did the debris come from, and 2) where will incoming debris go.

The first set of experiment was a forward trajectory run with a delayed release with the current as the flow field. Particles were kept at a constant surface depth of 0.25m. A delayed release is when an initialization point is set to release multiple particles at a particular interval in time. For this experiment, a particle was released once every three hours for the first 10 days of the simulation. Starting points (n=10) are represented by black stars in Figure 5a, and these were set at approximately 5-km offshore along the windward side of the island. This simulation ran for all 12 months for the years 2014, 2015, and 2016. Figure 5a shows the setup of the experiment.

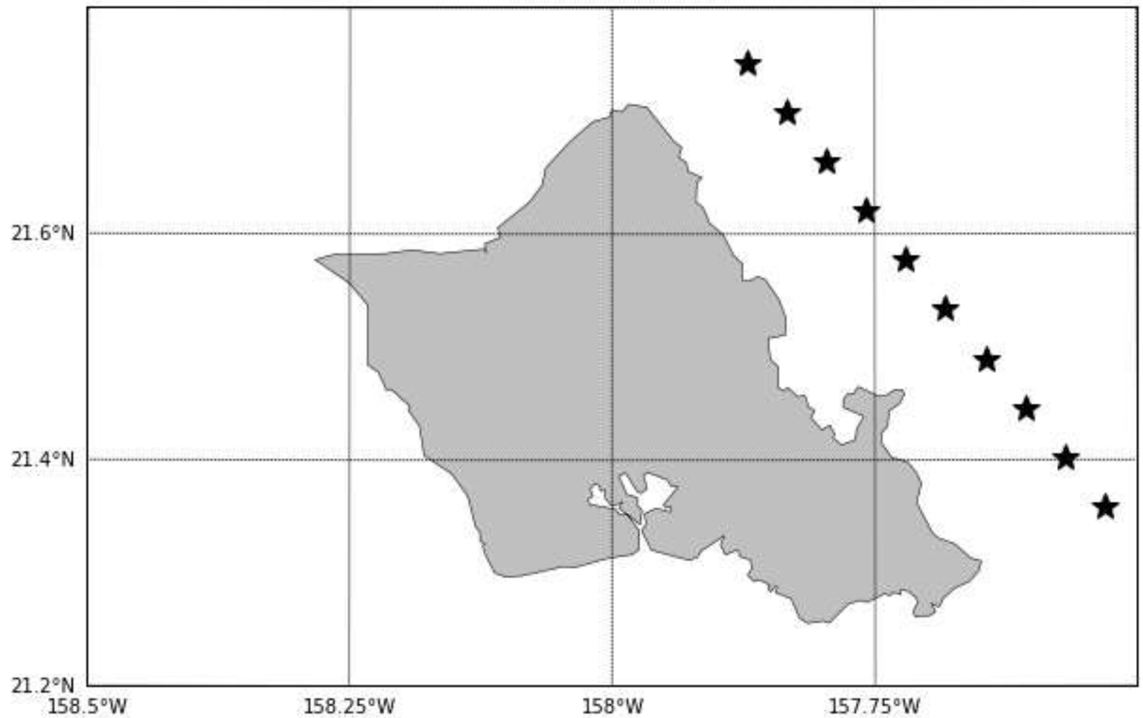

Figure 5a. Experiment set up for the first set of experiments. The black stars represent the starting point in which the particles will be released from.

The second set of experiments were done using a backward trajectory run with the currents as the flow field. Particles were again kept at a constant surface depth of 0.25m. Initialization points were moved from offshore and placed around the island, essentially mimicking the coastline. With a total of 44 starting points, the simulation ran for the first 10 days of every month for the years 2014, 2015, and 2016 with a timestep of 1 hour. See Figure 5b for experiment set up.

The third set of experiments were done using a backwards trajectory run with the tidal data as the flow field. Particles were kept at a constant surface depth. Initialization points and runtime are identical to the second experiment. However, this experiment only ran for the year of 2021. See Figure 5b for experiment set up.

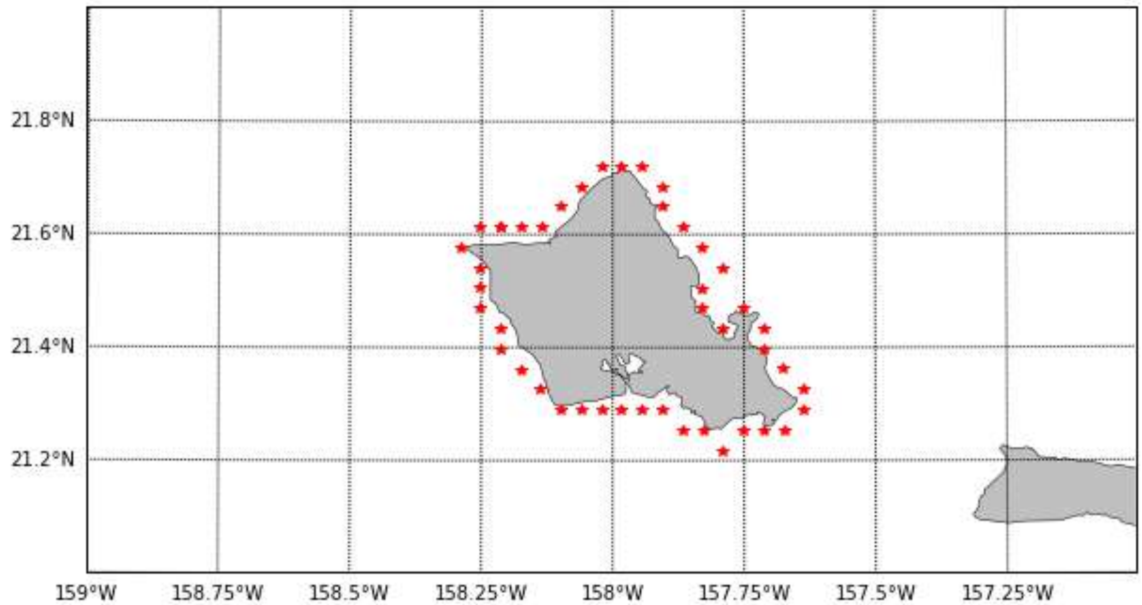

Figure 5b. Experiment set up for the second and third sets of experiments. Red stars are where the particles will be release from, representing the destination of debris.

4.0 Results

The results from all experiments are presented next. The analysis is divided into first looking at mean conditions (currents and tides) and then at the specific forward and backward trajectory runs.

4.1 Mean Conditions

4.1.1 Currents

Figure 6 shows the large-scale mean velocity conditions surrounding the Main Hawaiian Islands averaged over nine years (2008 – 2016). In these seasonal means, the North Hawaiian Ridge Current (NHRC), the Hawaiʻi Lee Current (HLC), and the North Equatorial Currents (NEC) are defined with slight variation in speed. However, the Hawaiʻi Lee Counter Current (HLCC) is only seen with definition in DJF (December, January, February).

There are eddies visible across all four panels with the months DJF and SON (September, October, November) having the most. Both DJF and SON have four eddies, with the most notable ones being a large, cyclonic eddy that sits back-to-back with a smaller anticyclonic eddy on the lee side of Hawai‘i Island. These two eddies are also seen in JJA (June, July, August), but only the anticyclonic eddy is visible in MAM (March, April, May).

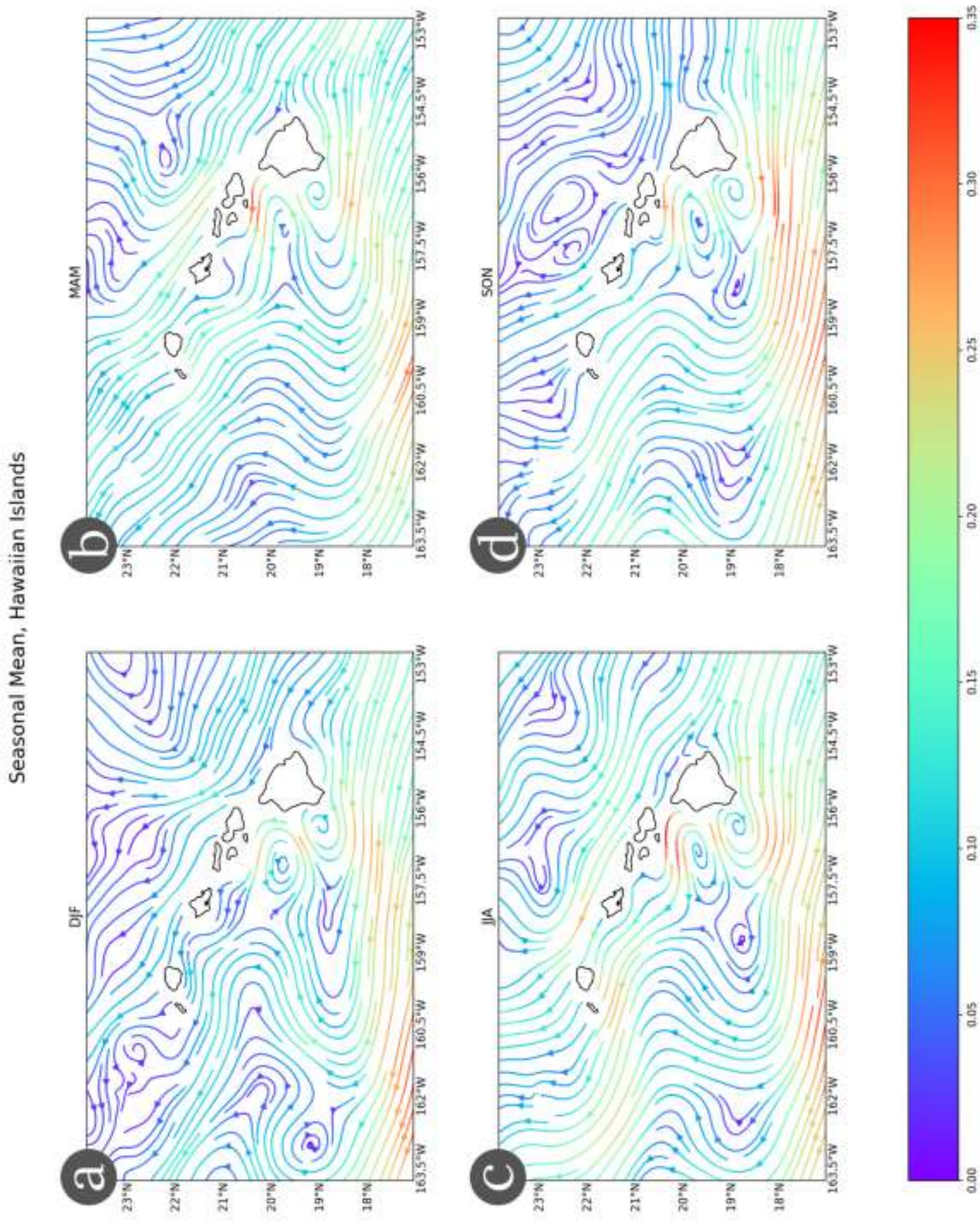

Figure 6. Seasonal mean conditions of large-scaled surface currents. Each panel shows a different season as indicated a) winter (December, January, February), b) spring (March, April, May), c) summer (June, July, August), and lastly, d) fall (September, October, November). Direction of the currents is show with the arrows and speed is represented by color.

4.1.2 Tides

The changes in tidal elevation and flow within a 24-hour period at an interval of 3 hours are shown in Figure 7. The first row shows the lowest tide of this particular day at 02:00 with a gradual increase in elevation at 05:00. At 02:00, there is a clear distinction between areas where the tide is lower and higher, with the highest tide at the time being in the southwest and south regions on the island, where the tidal currents are flowing in towards the southernmost region of the island. Meanwhile, the lowest tide of that time is in the northeast, where tidal currents are flowing up and around the northern most peak of the island. At 05:00, the tides are beginning to rise, with the northwest having the highest tide.

The second row are the times when tides are at their highest, finally being above mean sea level. At 08:00, tides are still relatively low around the island, which the sea surface height (SSH) being at around 0.00 to 0.15 meters, with higher tide being in the north and northeast. At 11:00, high tide is all around, with SSH being around 0.38 to 0.45 meters. At 14:00, the tide is dropping, with SSH being around 0.25 to 0.30 meters.

The last row shows tide dropping below sea level again. At 17:00, tides dip below sea level with SSH ranging around 0.0 to -0.0.50. At 20:00, SSH varies all over the island, with the lowest tide being at the southernmost point of the O’ahu at around -0.015 to -0.200 meters and the highest tides being on the northeastern side with SSH around -0.025 to 0.000 meters. At 23:00, the tides appear to be rising slightly, with the overall SSH being around -0.075 to 0.0 meters, with the northeast around mean sea level (0.0).

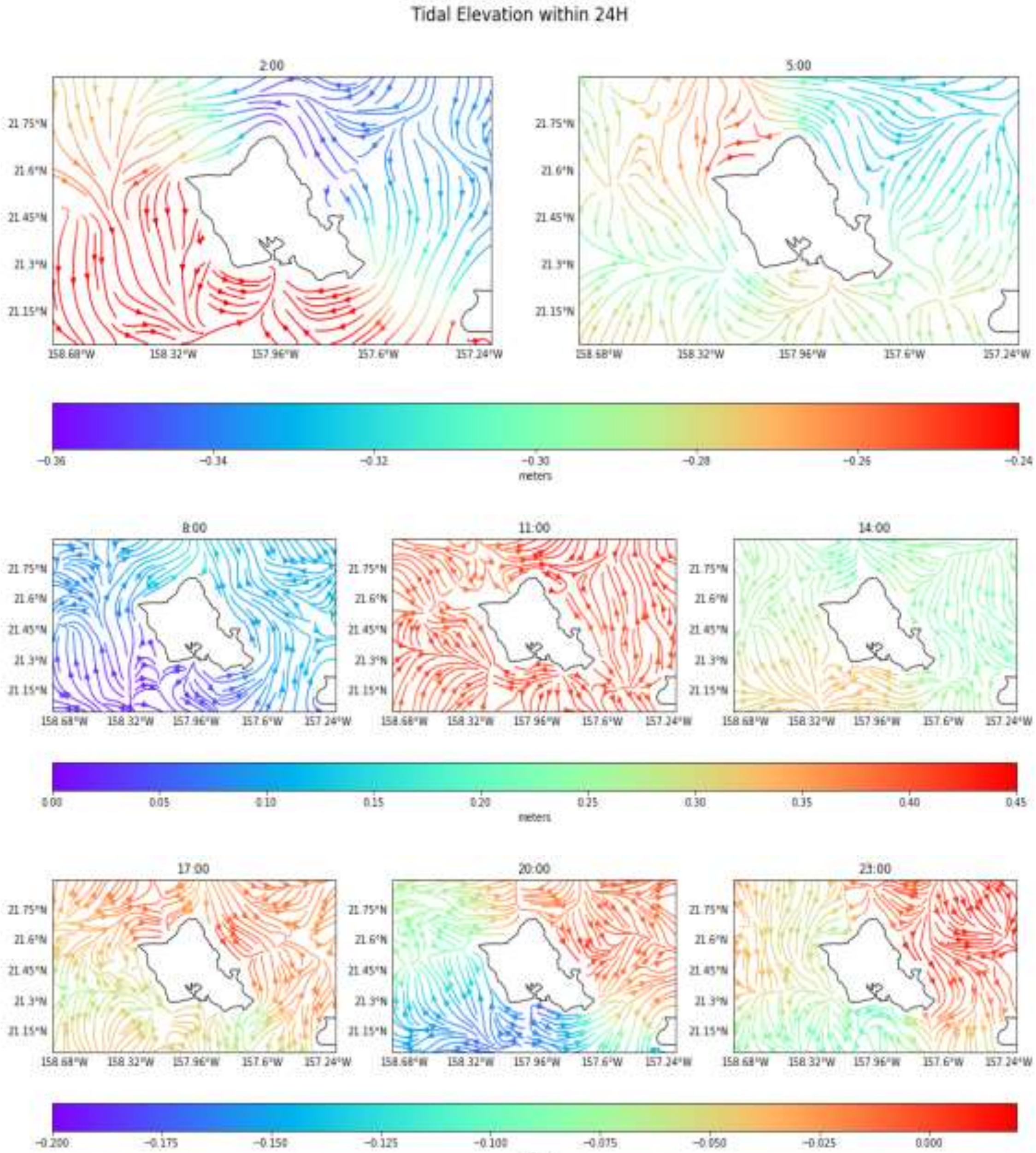

Figure 7. Changes in tidal elevation within a 24-hour period, shown at a 3-hour interval.

4.1.3 Speed and Directional Variance

Currents surrounding the MHI generally vary greatly in direction but quite little in speed. An exception to direction variance is the HLCC which directly affects the leeward side of Hawaiʻi Island. However, the general area off to the west of the leeward side of

Hawai‘i Island almost consistently high variance in speed. Datasets from 2008 to 2016 were used to calculate both direction and speed variances. Variances were calculated by averaging the squared deviation from the mean. Despite having a mean trade wind region, surface currents are still highly variable. The high variability in seen direction may, in part, explain why debris accumulates in an uneven manner.

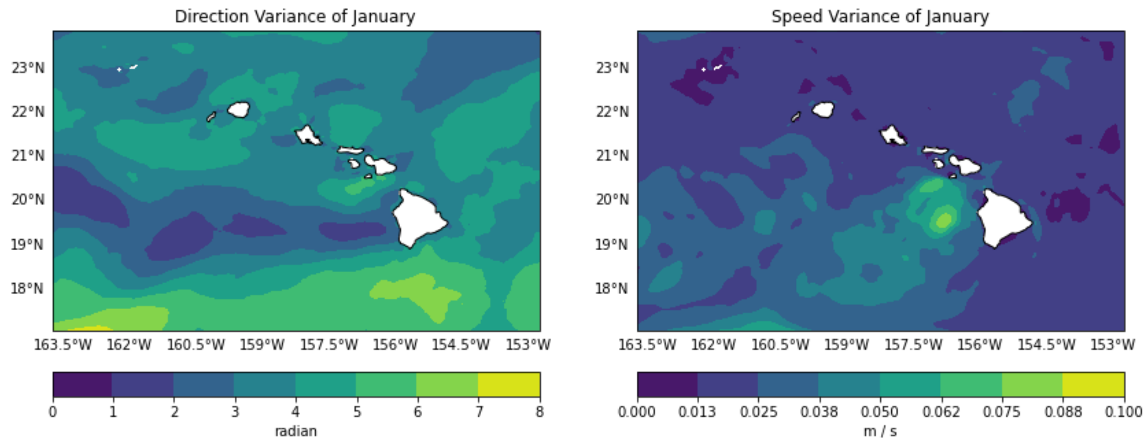

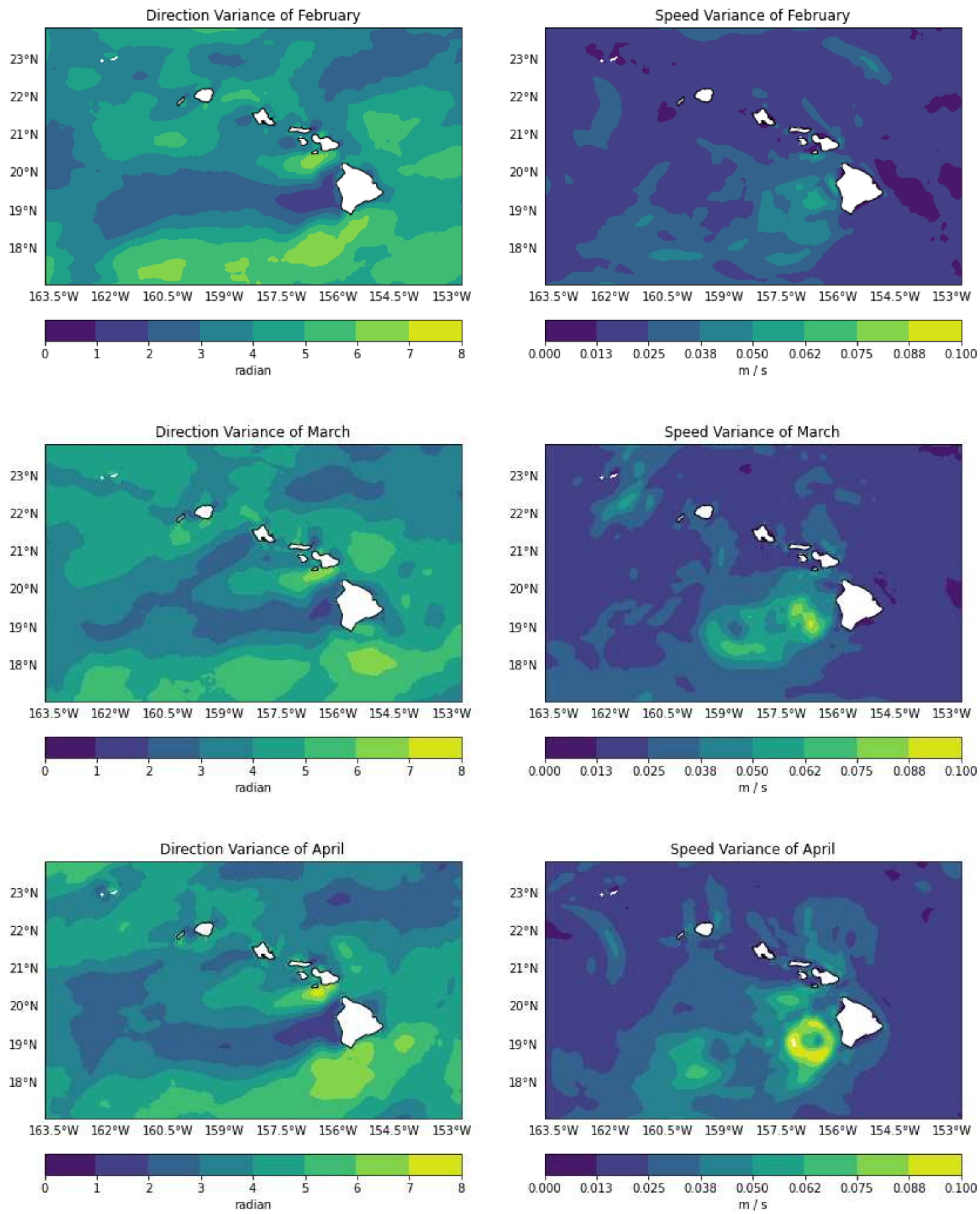
Direction Variance of February
Speed Variance of February
Direction Variance of March
Speed Variance of March
Direction Variance of April
Speed Variance of April
23°N
22°N
21°N
20°N
19°N
18°N
163.5°W
162°W
160.5°W
159°W
157.5°W
156°W
154.5°W
153°W
0 1 2 3 4 5 6 7 8
radian
0.000 0.013 0.025 0.038 0.050 0.062 0.075 0.088 0.100
m / s

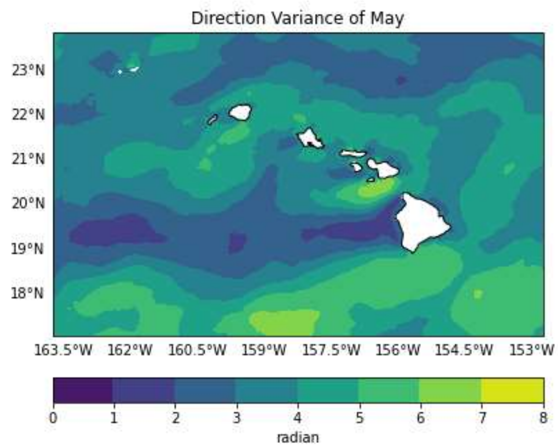
Direction Variance of May
23°N
22°N
21°N
20°N
19°N
18°N
163.5°W 162°W 160.5°W 159°W 157.5°W 156°W 154.5°W 153°W
0 1 2 3 4 5 6 7 8
radian

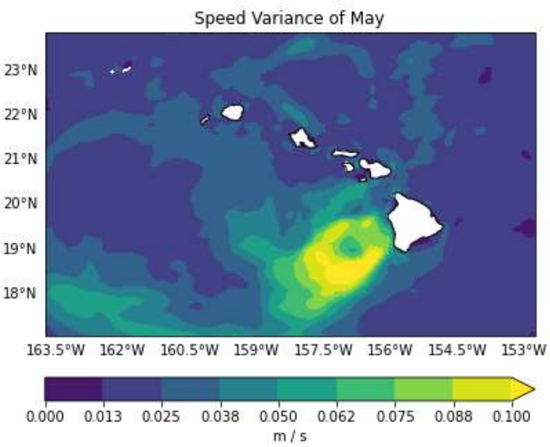
Speed Variance of May
23°N
22°N
21°N
20°N
19°N
18°N
163.5°W 162°W 160.5°W 159°W 157.5°W 156°W 154.5°W 153°W
0.000 0.013 0.025 0.038 0.050 0.062 0.075 0.088 0.100
m / s

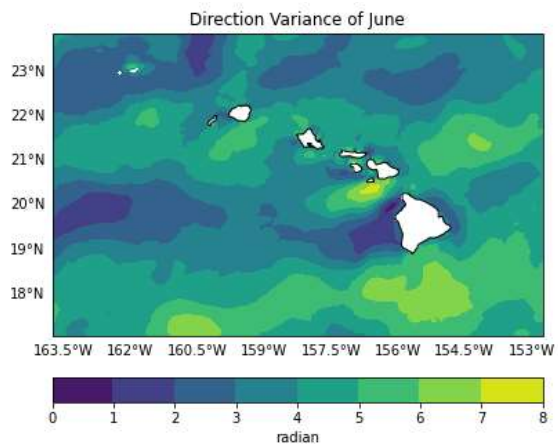
Direction Variance of June
23°N
22°N
21°N
20°N
19°N
18°N
163.5°W 162°W 160.5°W 159°W 157.5°W 156°W 154.5°W 153°W
0 1 2 3 4 5 6 7 8
radian

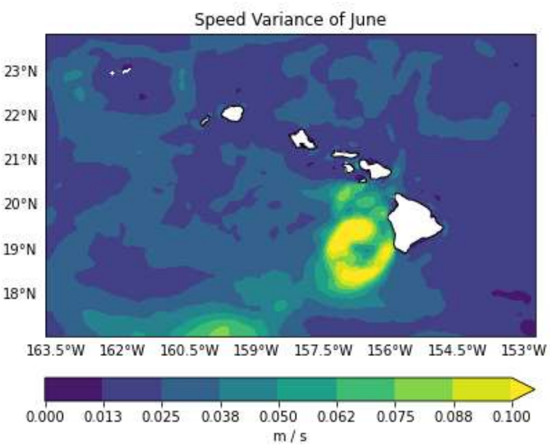
Speed Variance of June
23°N
22°N
21°N
20°N
19°N
18°N
163.5°W 162°W 160.5°W 159°W 157.5°W 156°W 154.5°W 153°W
0.000 0.013 0.025 0.038 0.050 0.062 0.075 0.088 0.100
m / s

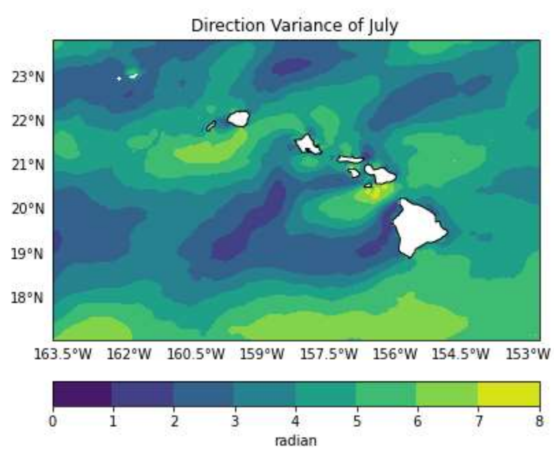
Direction Variance of July
23°N
22°N
21°N
20°N
19°N
18°N
163.5°W 162°W 160.5°W 159°W 157.5°W 156°W 154.5°W 153°W
0 1 2 3 4 5 6 7 8
radian

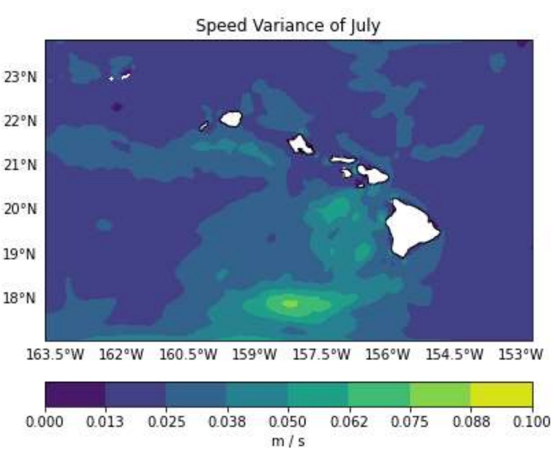
Speed Variance of July
23°N
22°N
21°N
20°N
19°N
18°N
163.5°W 162°W 160.5°W 159°W 157.5°W 156°W 154.5°W 153°W
0.000 0.013 0.025 0.038 0.050 0.062 0.075 0.088 0.100
m / s

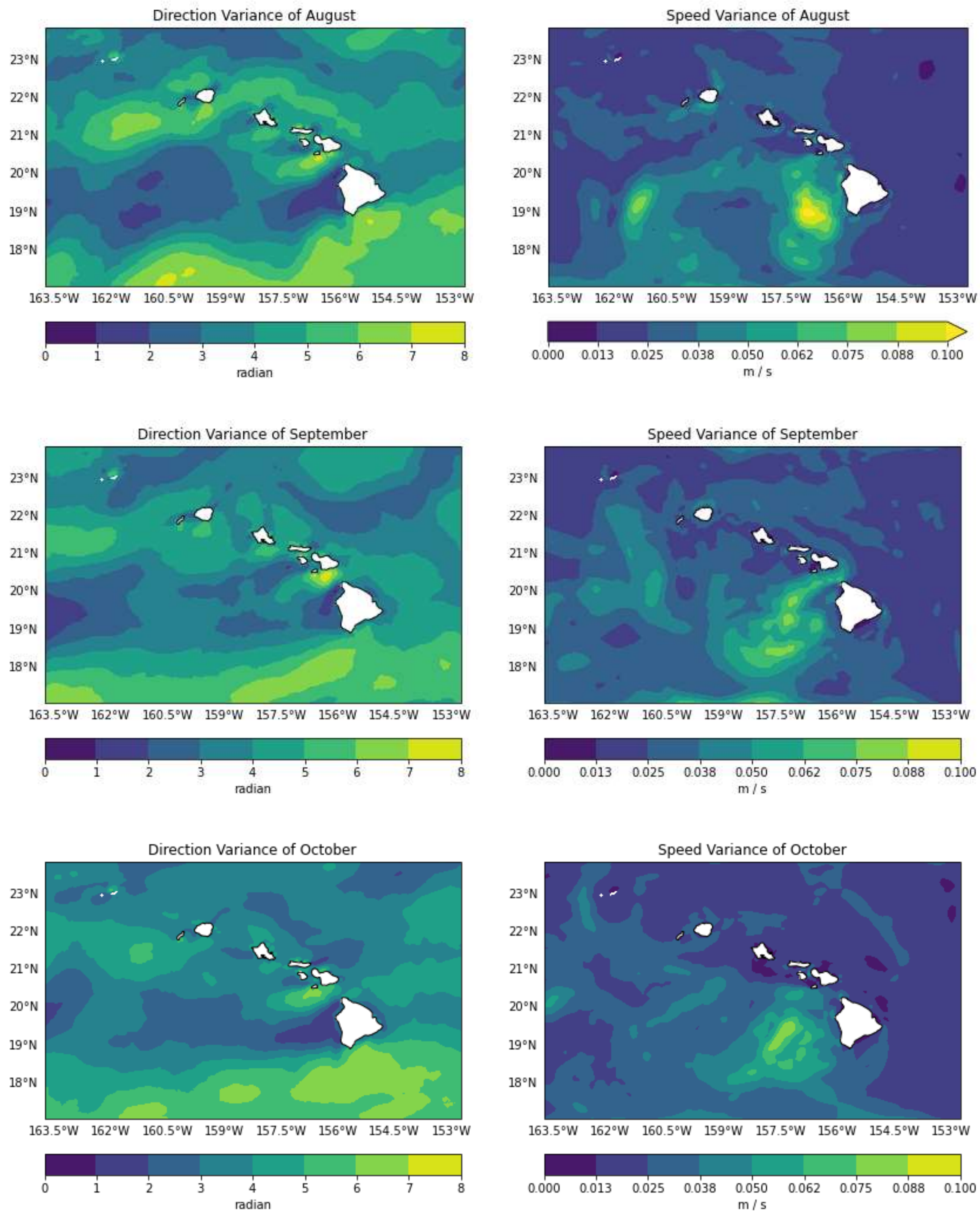
Direction Variance of August
Speed Variance of August
Direction Variance of September
Speed Variance of September
Direction Variance of October
Speed Variance of October
23°N
22°N
21°N
20°N
19°N
18°N
163.5°W 162°W 160.5°W 159°W 157.5°W 156°W 154.5°W 153°W
0 1 2 3 4 5 6 7 8
radian
0.000 0.013 0.025 0.038 0.050 0.062 0.075 0.088 0.100
m / s

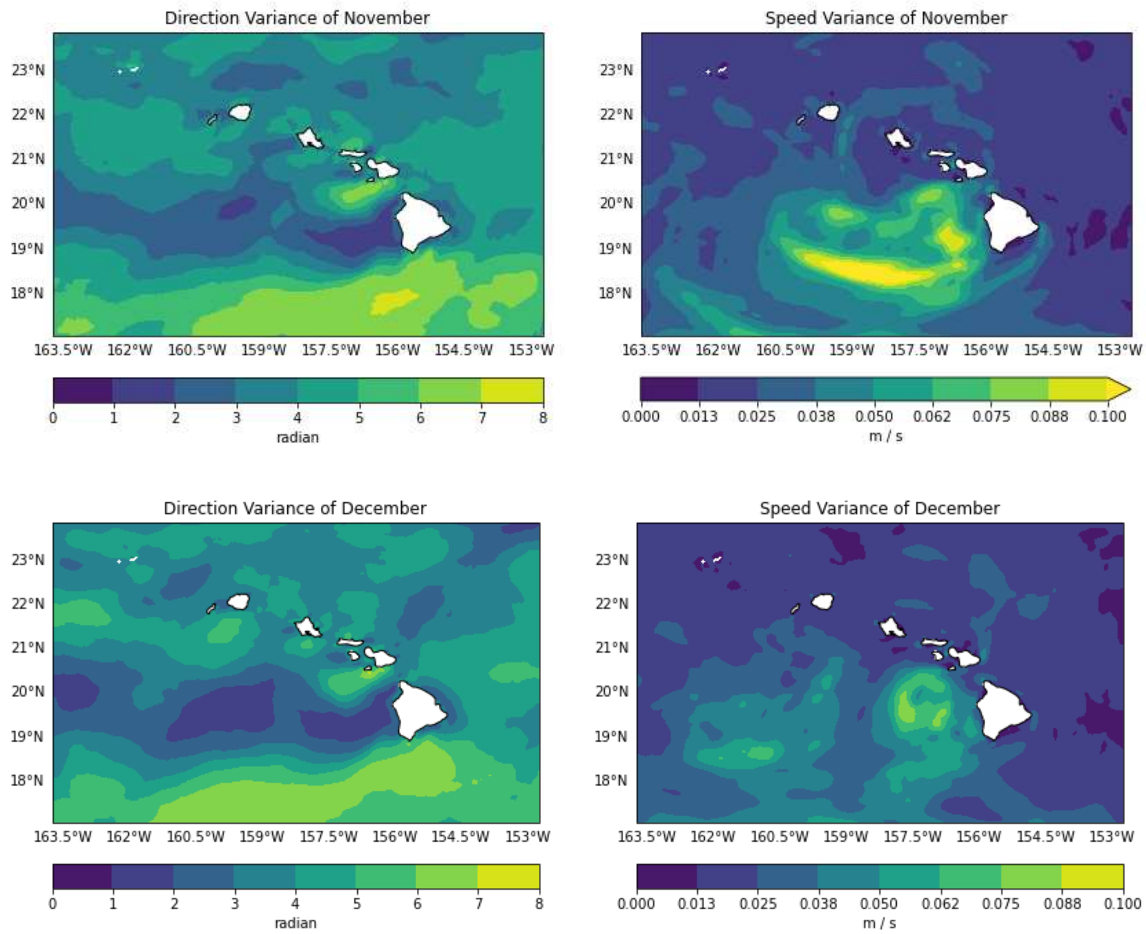

Figure 8. Monthly speed and directional variance of surface currents surrounding the Main Hawaiian Islands over a nine-year period (2008-2016).

4.2 Forward Trajectory

Figure 9 shows a comparison between the mean January currents around Oahu (Figure 9a) and trajectory results for individual months (January 2014, 2015, and 2016; Figure 9b, 9c and 9d, respectively). If the long-term mean were used as any sort of indication of incoming debris that were coming from the northeast, debris should not make landfall, as shown by the steady northwestward currents seen in the mean. However, that does not seem to be the case when looking at the individual runs. Particles do make landfall and in panels 9b and 9d and appear to head directly onshore. Panels 9b and 9c are also showing that the currents switched directions somewhere within the 10 days of the simulation. This is shown by the colors of certain particles existing closer to shore as well as further away from shore, past their initial starting points. The results from the forward trajectory simulation showed two things: 1) long-term seasonal means do not appear to be reliable for making predictions or drawings conclusions on the destination of incoming debris, and 2) destinations of incoming debris can vary greatly

Long-Term Mean VS the January's

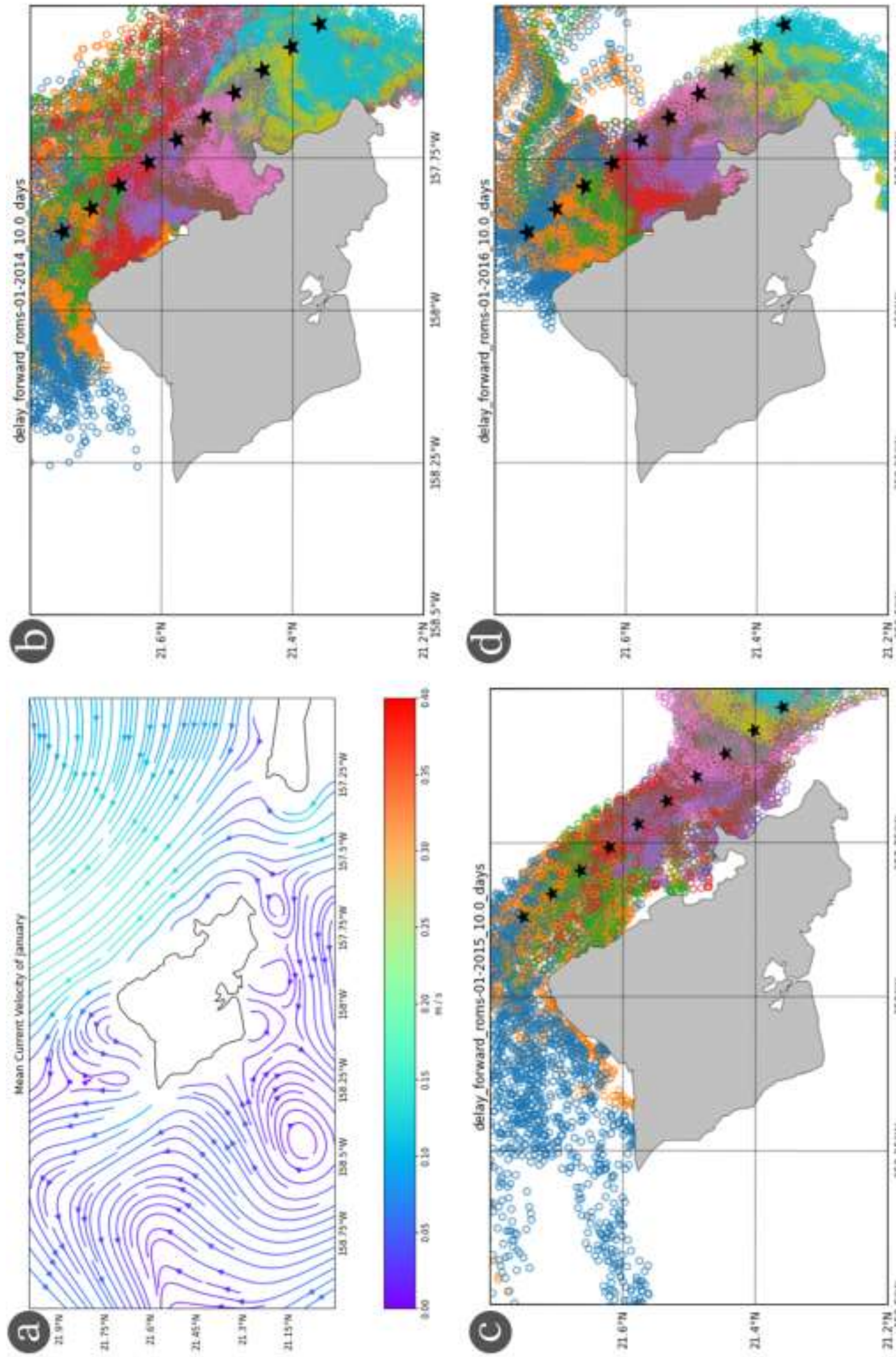

Figure 9. Comparison between the long-term seasonal mean for January and the forward trajectory simulation for the Januarys from b) 2014, c) 2015, and d) 2016.

Figure 10 shows that even individual months within the same year (2015) have currents that would transport debris in different ways. Panels 10a (January release), 10c (April release), and 10d (September release) all show particles making landfall, but where they do so vary, leaving some parts of the shore completely untouched by potential debris.

Forward Trajectory w/ Delayed Release, 2015

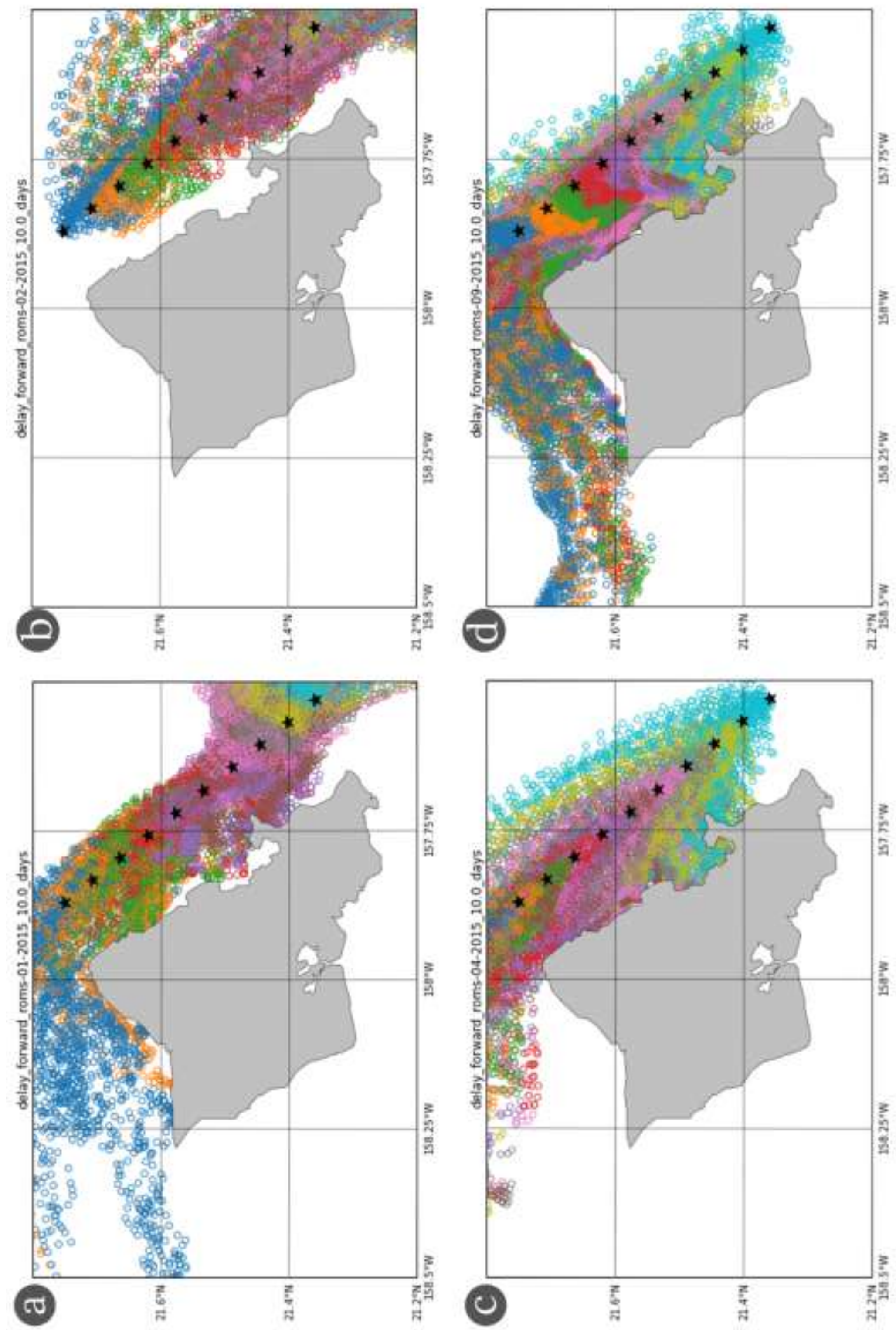

Figure 10. Forward trajectory simulations with a delayed release for the year 2014. Shown are four months: a) January, b) February, c) April, and d) September.

4.3 Backward Trajectory

4.3.1 Currents

No two runs were the same. Backward trajectories are used to simulate the debris origin (and path taken) before reaching their destination. The variations found could mean that the origin of incoming debris could be from a wide range of sources. Variabilities were found to exist between the same months of differing years (Figure 11a), between consecutive months within the same year (Figure 11b), and between the start and ending of the same month (Figure 11c). The result from these experiments all show that surface currents are highly variable.

Variations Between the January's of 2014, 2015, and 2016

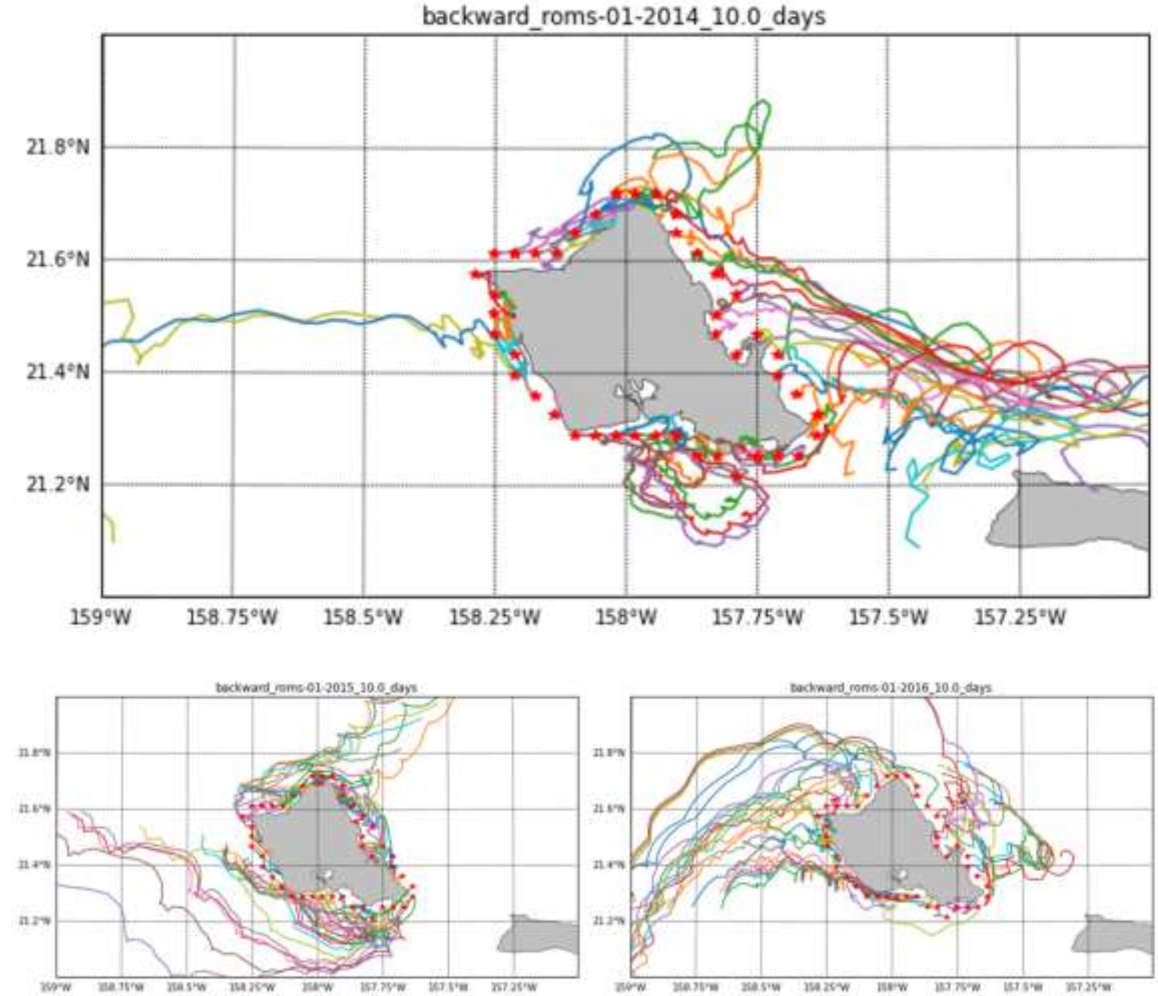

Figure 11a. Three different January's displaying three completely different trajectory paths. Top: January 2014. Bottom (from left to right): January 2015, January 2016.

Backward Trajectory, 2014

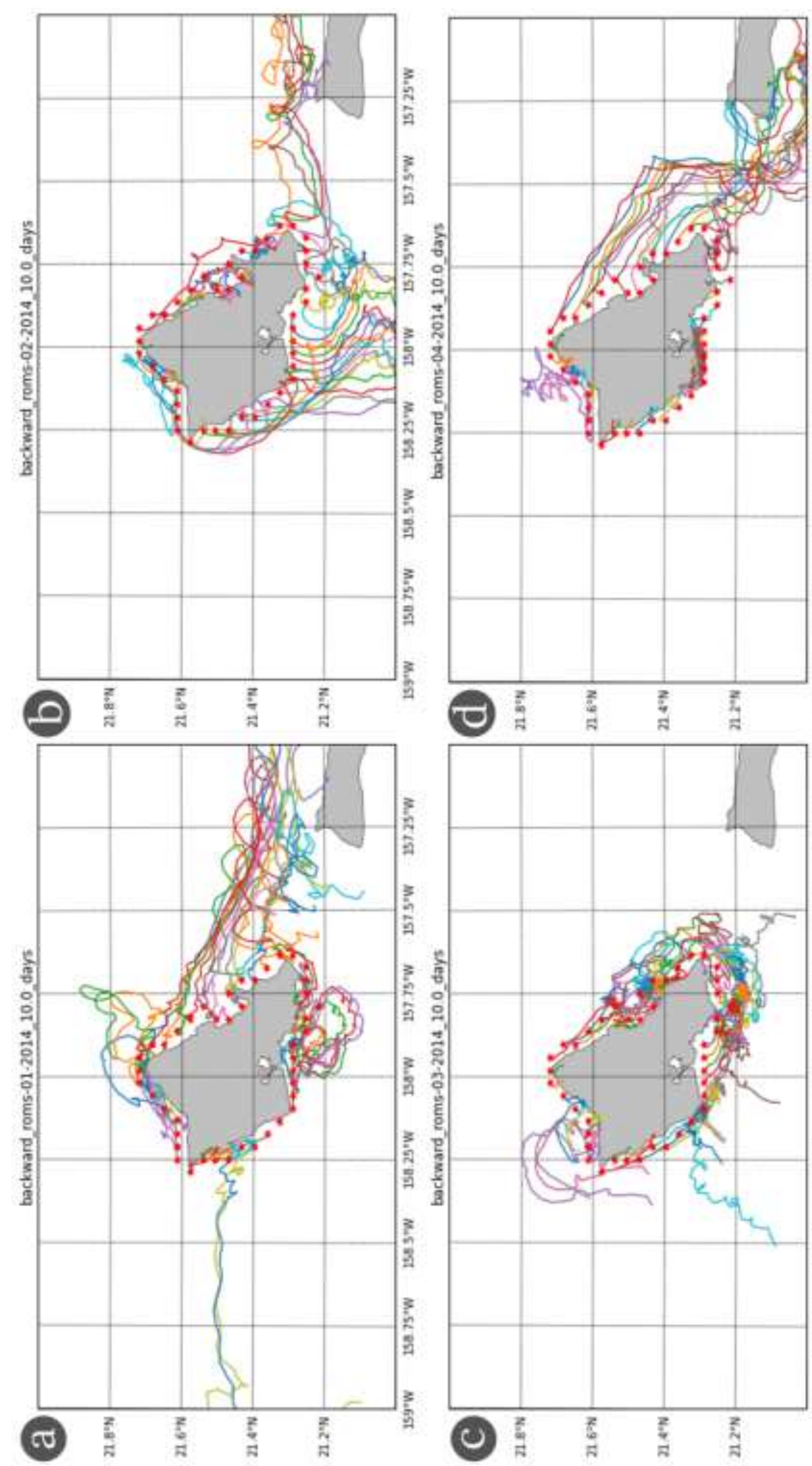

Figure 11b. Backward trajectory paths of four consecutive months starting from January to April 2014.

Beginning VS the End of January, 2016

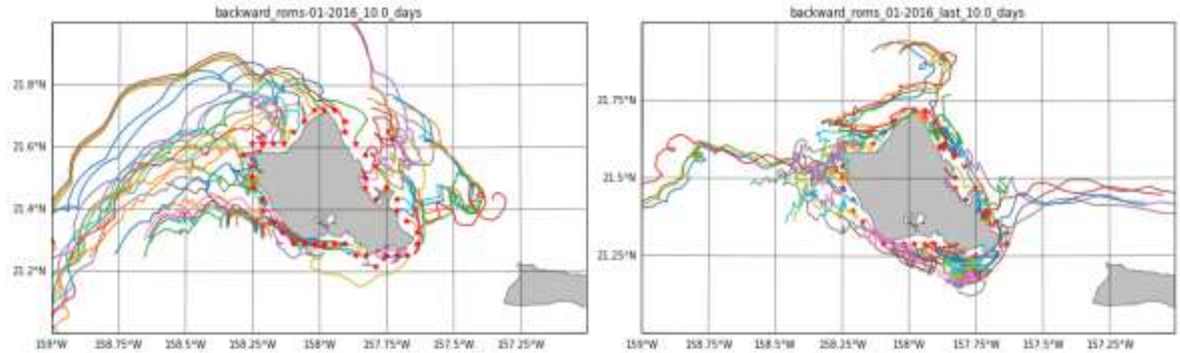

Figure 11c. Left: backward trajectory for the first ten days of January 2016. Right: backward trajectory for the last 10 days of January 2016.

4.3.2 Tides

Tidal influences on particles varied much less than the currents. Particles with initial release points on the northeastern side of the islands appears to move at a higher speed with nearly all figures showing particles being transported to the northernwest side of the island. Tidal action seems to only push particles back and forth along the shorelines with very little movement out towards sea.

Monthly Tidal Influences, 2021

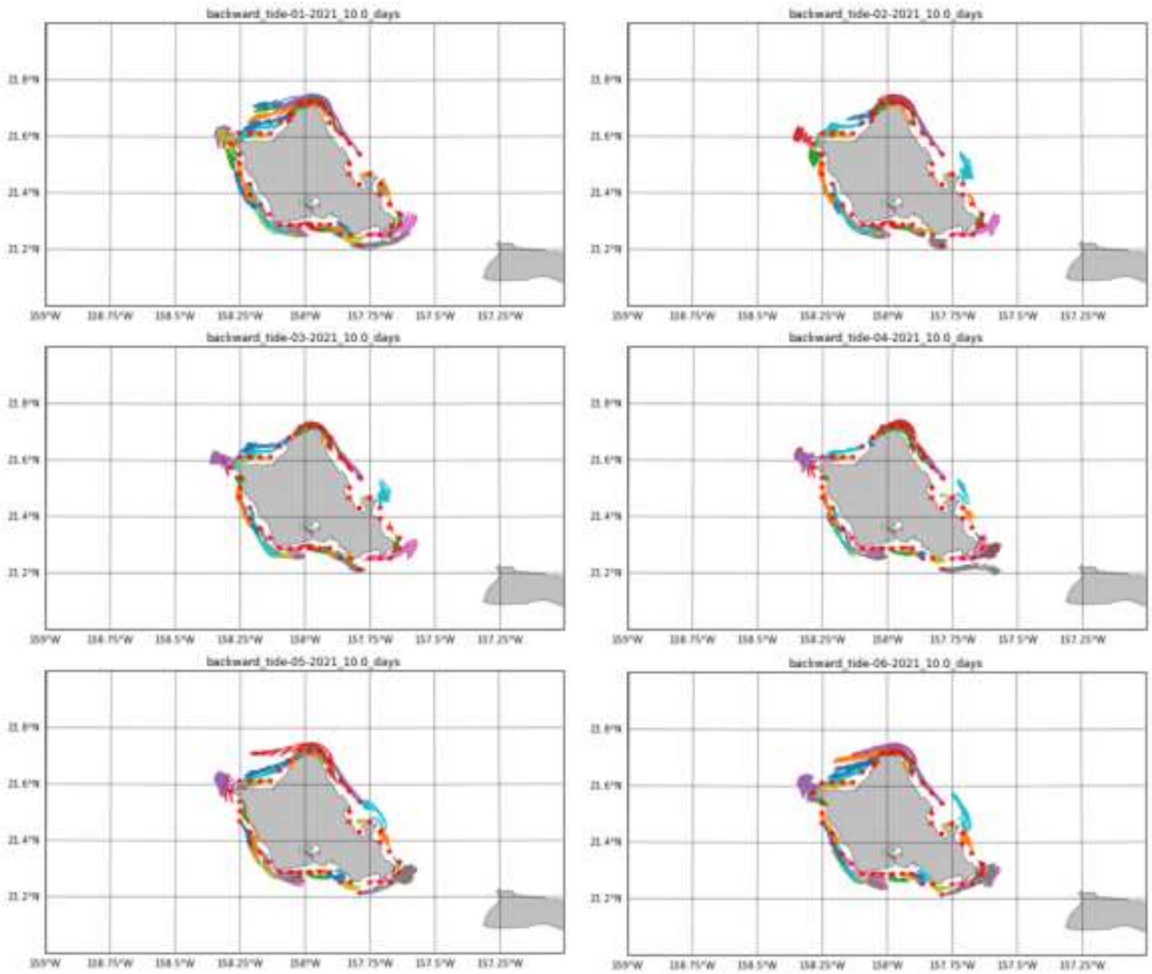

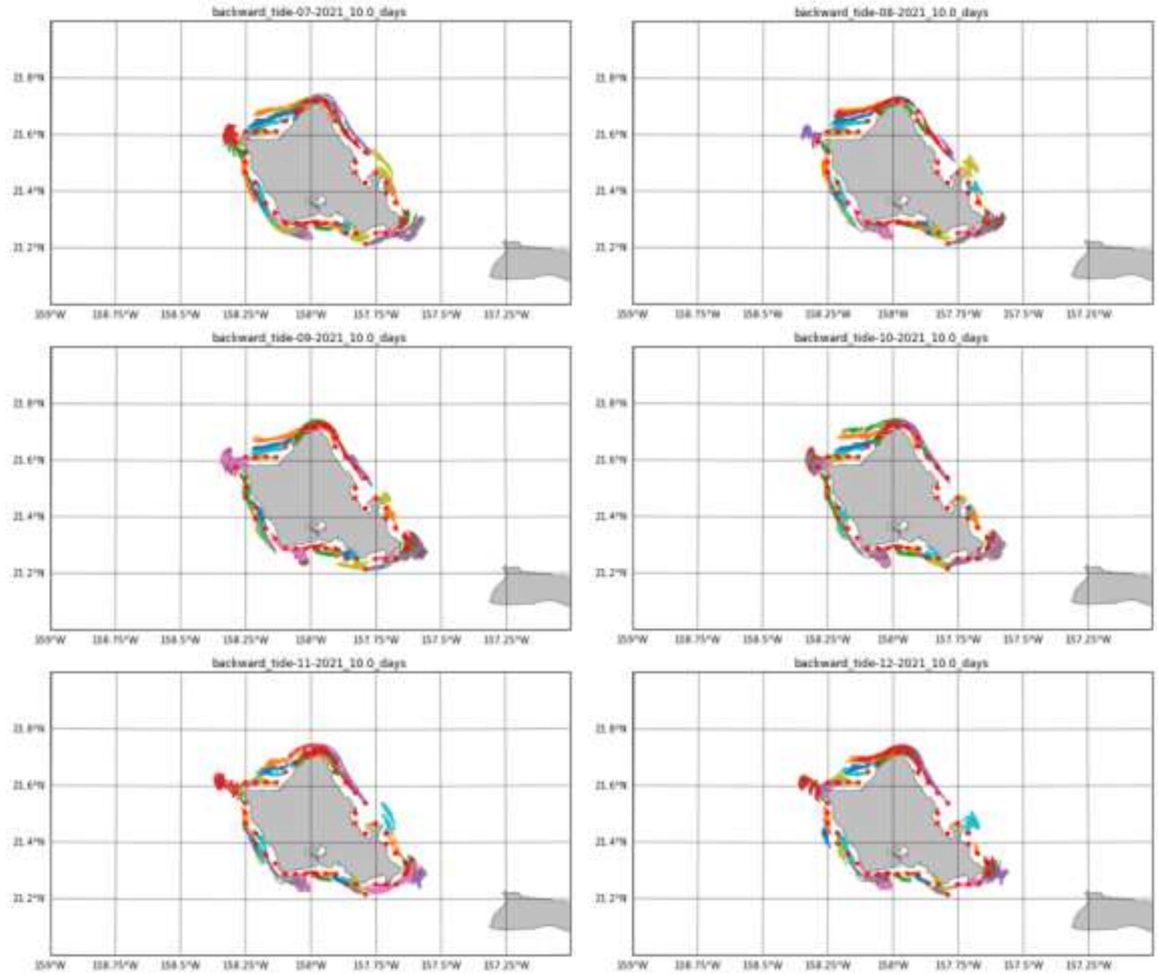

Figure 12. Monthly, 10-day backwards trajectory run with tidal influences for the year of 2021.

5.0 Conclusion

Two conclusions can be drawn from the results of this study: 1) seasonal mean conditions do not seem like they can be relied on to generate predictions or draw conclusions on the deposition rate of marine debris along the shorelines of O‘ahu, and 2) surface currents are highly variable and time dependent. While surface currents likely move debris on and offshore, tidal action seems to mainly push debris back and forth along shorelines. Due to its high spatial and temporal variability, surface currents could play a large role in the uneven deposition of marine debris along shorelines of O‘ahu.

6.0 Discussion

There some notable limitations to this study. Our study does not fully represent real world conditions as it does not take in account important factors such as windage, wave action, and debris that were able to change densities. While other studies like Critchell and Lambrechts (2016) included beaching, settling, resuspension/re-floating, windage, and distinctions between micro- and marco- plastics, our particles were kept at a constant surface level depth and size.

There is also a lack of reference date sets for debris accumulation. Moy et al. (2018) is a notable exception, and this provided a continuous distribution data set over the entire island at one time. However, since their survey was conducted between August to November of 2015, we cannot assume that their findings are representative of what the MHI shorelines look like on a daily basis. Furthermore, their debris density maps were made using the total amount of items found within the timeframe of their survey, which does not allow us to look at what debris deposition look like per month or day-to-day. Perhaps beach clean ups were done within their survey timeframe and that could drastically alter their data collection. There is also no distinction between where the debris had come from (land vs ocean sources).

While this study could be expanded to look at factors such as windage and changing debris density, more studies like Moy et al. (2018) are critical to better understand marine deposition patterns in Hawaii. Such studies would also help guide cleanup and mitigation efforts in the State.

LITERATURE CITED

Armstrong, R.W., 1983. Atlas of Hawaiʻi. Honolulu: University of Hawaiʻi Press, p. 54.

Blickley, L. C., Currie, J. J., & Kaufman, G. D. (2016). Trends and drivers of debris accumulation on Maui shorelines: Implications for local mitigation strategies. *Marine pollution bulletin*, *105*(1), 292-298.

Caldwell, P. C. (2005). Validity of north shore, Oahu, Hawaiian Islands surf observations. *Journal of Coastal Research*, *21*(6 (216)), 1127-1138.

Carlton, J. T., Chapman, J. W., Geller, J. B., Miller, J. A., Carlton, D. A., McCuller, M.I., and Ruiz, G. M. (2017). Tsunami-driven rafting: Transoceanic species dispersal and implications for marine biogeography. *Science*, *357*(6358), 1402-1406.

Carter, G. S., Merrifield, M. A., Becker, J. M., Katsumata, K., Gregg, M. C., Luther, D. S., Levine, M. D., Boyd, T. J., & Firing, Y. L. (2008). Energetics of M2 Barotropic-to-Baroclinic Tidal Conversion at the Hawaiian Islands, *Journal of Physical Oceanography*, *38*(10), 2205-2223. Retrieved Aug 20, 2021, from https://journals.ametsoc.org/view/journals/phoc/38/10/2008jpo3860.1.xml

Critchell, K., and Lambrechts, J. (2016). Modelling accumulation of marine plastics in the coastal zone; what are the dominant physical processes?. *Estuarine, Coastal and Shelf Science*, *171*, 111-122.

Delandmeter, P., and van Sebille, E. V. (2019). The Parcels v2. 0 Lagrangian framework: new field interpolation schemes. *Geoscientific Model Development*, *12*(8), 3571-3584.

English, E., Wagner, C., and Holmes, J. (2019). The Effects of Marine Debris on Beach Recreation and Regional Economies in Four Coastal Communities: A Regional Pilot Study. *Final Report*.

Giambelluca, T.W. and Schroeder, T.A., (1998). Climate. In: Juvik, S.P., and Juvik, J.O. (eds.), Atlas of Hawai„i. Honolulu: University of Hawai„iPress, pp. 49-59.

Hawaii Tourism Authority (HTA) (2019*). 2019 Annual Visitor Research Report* (HTA Release (20-03)). Hawaiʻi Tourism Authority. https://www.hawaiitourismauthority.org/media/5062/2019-annual-report-final-for-posting.pdf

Howell, E. A., Bograd, S. J., Morishige, C., Seki, M. P., and Polovina, J. J. (2012). On North Pacific circulation and associated marine debris concentration. *Marine Pollution Bulletin*, *65(1-3), 16-22.*

Jambeck, J. R., Geyer, R., Wilcox, C., Siegler, T. R., Perryman, M., Andrady, A., Narayan, R., & Law, K. L. (2015). Marine pollution. Plastic waste inputs from land into the ocean. *Science (New York, N.Y.)*, *347*(6223), 768–771. https://doi.org/10.1126/science.1260352

Jang, Y. C., Hong, S., Lee, J., Lee, M. J., and Shim, W. J. (2014). Estimation of lost tourism revenue in Geoje Island from the 2011 marine debris pollution event in South Korea. *Marine pollution bulletin*, *81*(1), 49-54.

Lange, M., and Sebille, E. V. (2017). Parcels v0. 9: prototyping a Lagrangian ocean analysi Analysis framework for the petascale age. *Geoscientific Model Development*, *10*(11), 4175-4186.

Lebreton, L., Greer, S., and Borrero, J., 2012. Numerical modelling of floating debris in the World's Oceans. Mar. Pollut. Bull. 64, 653-661.

Maximenko, N. and Hafner, J., 2012. Marine debris from the tsunami of March 11, 2011: one year after the disaster. In: Presentation at the International Pacific Research Center, Honolulu, HI.

Ministry of the Environment, Government of Japan, (2012) Ministry of the Environment, Government of Japan Estimated Total Amount of Debris Washed out by the Great East Japan Earthquake http://www.kantei.go.jp/jp/singi/kaiyou/hyouryuu/pdf/souryou_eng.pdf

Moy, K., Neilson, B., Chung, A., Meadows, A., Castrence, M., Ambagis, S.,and Davidson, K. (2018). Mapping coastal marine debris using aerial imagery and spatial analysis. *Marine pollution bulletin*, *132*, 52-59.

NOAA Marine Debris Program (2014a) Report on the Entanglement of Marine Species in Marine Debris with an Emphasis on Species in the United States. Silver Spring, MD. 28 pp

NOAA Marine Debris Program (2014b) Report on the Occurrence and Health Effects of Anthropogenic Debris Ingested by Marine Organisms. Silver Spring, MD. 19 pp

Partridge, D., Friedrich, T., and Powell, B. S. (2019). Reanalysis of the PacIOOS Hawaiian Island Ocean Forecast System, an implementation of the Regional Ocean Modeling System v3. 6. *Geoscientific Model Development*, *12*(1), 195-213.

Reisser, J., Shaw, J., Wilcox, C., Hardesty, B.D., Proietti, M., Thums, M., and Pattiaratchi, C., 013. Marine plastic pollution in waters around Australia: characteristics, concentrations, and pathways. PloS One 8, e80466.

Ribic, C. A., Sheavly, S. B., Rugg, D. J., and Erdmann, E. S. (2012). Trends in marine debris along the US Pacific Coast and Hawai'i 1998–2007. *Marine Pollution Bulletin*, *64*(5), 994-1004.

Rooney, J. and Fletcher, C.H., (2005). Shoreline Change and Pacific Climatic Oscillations in Kihei, Maui, Hawaiʻi. Journal of Coastal Research, 21(3), 535-547.

Ruiz, G. M., Carlton, J. T., Grosholz, E. D., and Hines, A. H. (1997). Global invasions of marine and estuarine habitats by non-indigenous species: mechanisms, extent, and consequences. *American zoologist*, *37*(6), 621-632.

Sebille, Erik, Aliani, Stefano, Law, Kara, Maximenko, Nikolai, Alsina, J., Bagaev, Andrei, Bergmann, Melanie, Chapron, Bertrand, Chubarenko, Irina, Cózar, Andrés, Delandmeter, Philippe, Egger, Matthias, Fox-Kemper, Baylor, Garaba, Shungudzemwoyo, Goddijn-Murphy, Lonneke, Hardesty, Britta, Hoffman, M. , Isobe, Atsuhiko, Jongedijk, Cleo and Wichmann, David. (2020). The physical oceanography of the transport of floating marine debris. Environmental Research Letters. 15. 10.1088/1748-9326/ab6d7d.

United States Environmental Protection Agency. *Sources of Aquatic Trash*. Retrieved: July 22, 2021 from https://www.epa.gov/trash-free-waters/sources-aquatic-trash

Vitousek, S., Barbee, M. M., Fletcher, C. H., Richmond, B. M., and Genz, A. S. (2009). Puʻukohola–Heiau National Historic Site and Kaloko-Honoko–hau Historical Park, Big Island of Hawaiʻi. *Coastal Hazard Analysis Report. NPS Geologic Resources Division, Honolulu, HI*.

Wyrtki, K., and Graefe, V. (1967). *Approach of tides to the Hawaiian Islands. Journal of Geophysical Research, 72(8), 2069–2071*. doi:10.1029/jz072i008p02069